Tunable Microfluidic Optical-Fiber Devices Based on Electrowetting Pumps and Plastic Microchannels

J. Hsieh, P. Mach, F. Cattaneo, S. Yang, T. Krupenkine, K. Baldwin, and J. A. Rogers

***Abstract*—This letter introduces a class of tunable microfluidic fiber device that uses molded plastic microchannels and electrowetting pumps. It demonstrates the application of this type of system to dynamically adjustable narrow-band and wide-band all-fiber filters. Compact size, low-cost fabrication procedures, low-power (<1 mW) consumption, nonmechanical operation, and good optical characteristics are among the attractive features of these devices. They have many attributes that could make them useful for certain applications in photonics.**

***Index Terms*—Fluidics, gratings, micropumps, optical-fiber devices, optical waveguide components.**

I. INTRODUCTION

TUNABLE optical-fiber devices can be useful for many important operations in optical communication systems: dynamic chromatic dispersion compensation, programmable adding and dropping of wavelength channels, dynamic-gain equalization, etc. Nearly all of these components are tuned simply by exploiting thermo-optic or strain-optic effects in the silica of the fiber. Approaches for using pumped fluids to dynamically tune the transmission characteristics of optical fiber are more recent [1]–[3]. These techniques increase the range and type of tunability that can be achieved. They can also be easily combined with the more traditional thermal and strain based techniques to enable complex and multifunctional tuning. For example, thermal pressure pumping and thermo-optic tuning of microfluidic plugs in microstructured, or "holey," fiber yields tunable wide and narrow-band all-fiber filters [1]. Another type of fluidic device uses electrowetting pumps and planar bulk-machined fluid channels with conventional fiber to achieve similar functionality [3]. This system is attractive because it does not require specialized fiber, it offers low power, latchable operation, and it provides flexible configurations that enable many forms of tuning that cannot be achieved easily with "holey" fiber.

In this letter, we describe and demonstrate a new design for electrowetting-based devices that offers many important advantages: it enables improved optical and switching characteristics in a low-cost miniaturized system that is compatible with use in fiber arrays, planar waveguides, and other small-scale optical systems. We begin by describing the design and operation of these devices followed by simple high-resolution molding approaches for fabricating them. We then illustrate their use with conventional long-period gratings and etched fibers to produce fast, widely tunable narrow- and broad-band fiber filters.

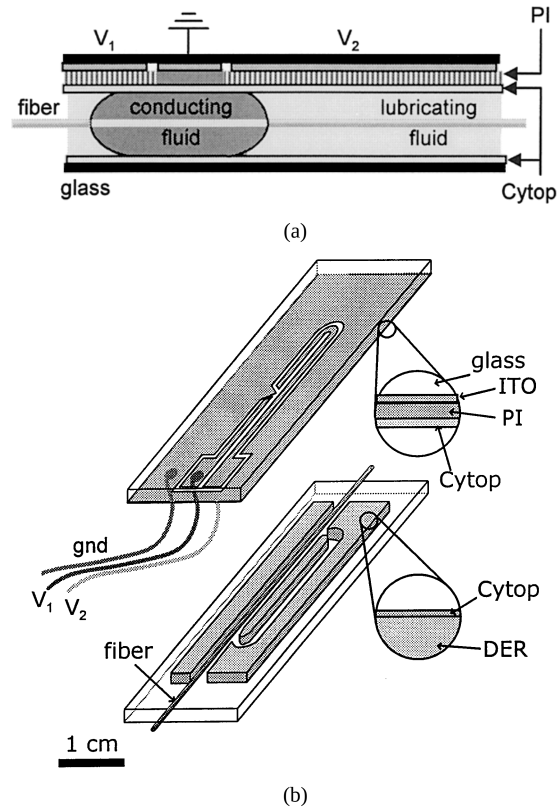

Fig. 1. (a) Cross-sectional schematic side view of the microfluidic channel and the electrodes for the electrowetting pump. (b) Angled, exploded view of the integrated system. The top substrate supports the electrowetting pump and the bottom substrate supports a micromolded layer of plastic that defines the microfluidic racetrack channel.

II. DEVICE DESIGN AND FABRICATION

The microfluidic components described here involve an optical fiber that lies in a straight section of a microfluidic channel in an oval "racetrack" configuration. An electrowetting pump dynamically controls the position of a microfluidic plug relative to a fiber section whose optical properties are sensitive to overlap with this fluid. The microfluidic part of this device consists of two separate elements: one substrate that supports a thin layer of micromolded plastic that defines the microfluidic channels, and another substrate that supports the electrodes that form the basis of the electrowetting pump (see Fig. 1). Fabrication of the microchannel substrate begins with photolithography to create patterns that have the required geometries in

Manuscript received August 26, 2002.
The authors are with Bell Laboratories, Lucent Technologies, Murray Hill, NJ 07974 USA.
Digital Object Identifier 10.1109/LPT.2002.805865

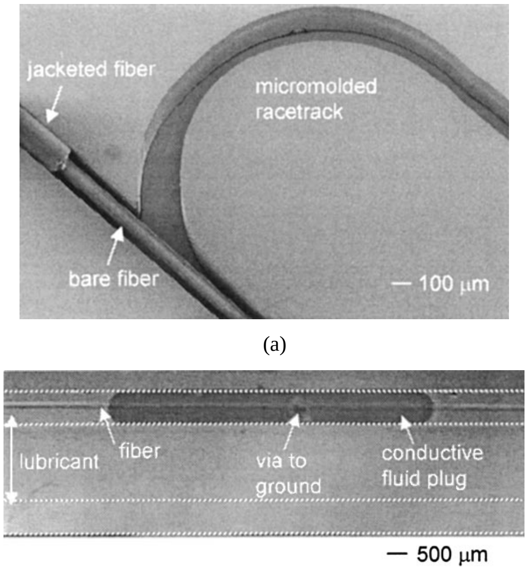

(b)

Fig. 2. (a) Scanning electron micrograph of an angle view of the micromolded racetrack. (b) Optical micrograph of a top view of a similar device, after filling with fluids and sealing the cell with the transparent top electrode substrate.

$\sim$300- to 350-μm-thick layers of a negative photoresist (SU-8 2100; Microchem Corp.) on glass slides. The racetrack layouts that we explored have various channel widths (250, 500, and 700 μm) and lengths (3, 4.5, and 6.5 cm). One straight side of the racetrack extends beyond the ends of the oval to accommodate the fiber. In the 250-μm-wide channel system, the jacketed part of the fiber fits snugly into the ends of this part of the channel, and naturally centers the stripped region of the fiber (see Fig. 2). Casting and curing a prepolymer of poly-dimethylsiloxane [(PDMS), Sylgard 184; Dow Chemical] against these photolithographically defined "masters" produces elastomeric molds in the geometry of the patterned resist. Contacting one of these molds with a thin layer of photocurable epoxy novolac resin [(DER) 354; Dow Chemical] on a glass slide, and then passing ultraviolet light through the mold cures and solidifies the DER in the geometry of the relief on the PDMS. Peeling the mold away yields a high quality plastic replica of the master. A single master can be used to form many molds, and each mold can be used many times. Dip coating the micromolded-DER channels in a fluoropolymer (Cytop; Asahi Glass) produces a hydrophobic surface that enables smooth pinning-free flow of the fluids.

The other substrate supports all three electrodes for the electrowetting pump. One of these electrodes (the common electrode) connects directly to the conducting microfluidic plug which is pumped by electrowetting. The other two are capacitatively coupled to opposite ends of this plug. Applying different voltages (V_1 and V_2) to these electrodes, while holding the common electrode (and therefore the plug itself) at ground, provides an electrowetting driving force, which is based on the different contact angles that develop at the two ends of the plug. The magnitude of this driving force is proportional to $(V_1 - V_2)^2$ [4]. The plug flows at a terminal speed that is determined by the balance of the electrowetting force against the various sources of drag.

The overall geometry of these electrodes matches that of the molded microchannel racetrack. Two of them run along the entire length of the racetrack. The common electrode enters the area of the racetrack at the location where the other two electrodes terminate, near the midpoint of the straight region that accommodates the fiber (see Fig. 1). The substrate is glass, and the electrodes are indium tin oxide (ITO) ($\sim$100-nm thick) patterned by photolithography and etching in concentrated HCl. A spin coated layer of polyimide ($\sim$2-μm-thick film of Durimide 32A, Arch Chemicals) provides an insulating layer on top of these electrodes; a 1-μm layer of Cytop spin coated on the polyimide produces the necessary hydrophobic surface. The Cytop and polyimide layers are removed at rectangular contact pads in the ITO at one edge of the substrate. Wires attach to these pads with indium solder and connect the electrodes to an external power supply. A small "via" hole near the location where the three electrodes meet enables electrical connection of the common electrode to the conducting fluid plug.

Mechanically clamping and/or gluing these two substrates together forms a microfluidic cell with integrated electrowetting pump. Filling the channels with a low surface energy lubricating fluid (polydimethylsiloxane (DMS-T00); Gelest, Inc.) facilitates flow. Due to its low surface energy, it is energetically favorable for the lubricating fluid to penetrate between the channel walls and the liquid plug, thus replacing a single solid-liquid interface with the liquid-fluid and solid-fluid interfaces. This leads to the creation of a thin lubricating layer that effectively isolates the liquid plug from the channel walls and thus substantially reduces stick-slip and contact angle hysteresis. Microcapillary syringes provide a convenient means to introduce a conducting fluid plug (aqueous solutions of $Na_2Cr_2O_7 \cdot 2\ H_2O$) with desired length. The concentration of the sodium chromate was chosen either to achieve an index of refraction equal to (58 weight percent) or higher (65 weight percent; index $\sim$1.50) than silica. Fig. 2(b) shows a top view of a portion of an assembled filled cell with a fiber in place. These devices allow reversible pinning-free voltage-controlled motion of the conducting plug at speeds of up to $\sim$1.8 cm/s for differential voltages of 100 V. The different channel geometries show similar performance. A hydrophobic fluorinated silane monolayer on the fiber's silica surface (formed by vapor-phase exposure to tridecafluoro-(1,1,2,2,tetrahydrooctyl)-1-trichlorosilane for $\sim$1 h; UCT, Inc.) eliminates any tendency for droplets of the conducting fluid to remain on the fiber when the fluid is pumped back and forth.

III. Results and Discussion

This letter demonstrates the use of this type of microfluidic system for two tunable-fiber devices: adjustable narrow-band and wide-band filters. The narrow-band device incorporates a long period fiber grating [5] [(LPG) 1.5 cm long, 362-μm period; O/E Land, Inc.] and an index-matched microfluidic plug. Matching the index of the fiber's surroundings to the fiber itself reduces the depth of the LPG resonance by eliminating the fiber-cladding modes. Partial overlap of such a fluid with the grating partially decreases the depth. The fluidic system described above provides a convenient and dynamic means for ad-

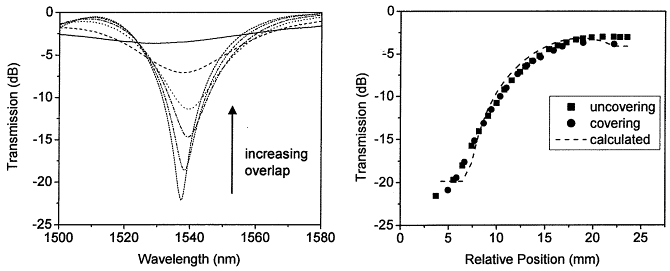

(a) (b)

Fig. 3. (a) Transmission spectrum of a long period fiber grating as an index-matched microfluidic plug is pumped into overlap with the stripped region of the fiber that contains grating. (b) Shows this depth as a function of the position of the edge of the fluid plug relative to a reference mark in the channel, recorded as the fluid was pumped into (covering) and out of (uncovering) overlap with the grating. The dashed line presents the results of a simple calculation that qualitatively describes the behavior.

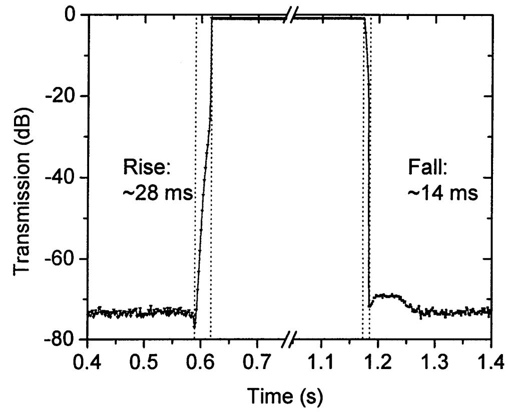

Fig. 4. Switching characteristics of a fluidic device that uses a fiber with a short (∼5 mm), uniformly etched region (diameter down to ∼13 μm) along its length.

justing the degree of overlap, and therefore the depth of the attenuation feature associated with the resonance. Fig. 3 presents data collected from tuning this device. The depth of the filter changes monotonically with increasing fluid overlap. Data collected as the fluid is pumped into and out of overlap with the grating demonstrates full reversibility and the absence of hysteresis. The behavior of the filter strength (i.e., transmission at the peak of the attenuation) with fluid overlap can be approximated by assuming that the grating couples to two different independent cladding modes: one guided mode associated with the region of the grating that is not in overlap with the index-matching fluid and one weakly guiding or leaky mode associated with the section in overlap. In this case, we treat the two sections of the grating as independent LPGs each of which contributes to transmission loss. For simplicity, we neglect detuning and other potentially important effects. The core-to-cladding mode coupling coefficients for the grating in these respective areas are κ_o and κ, where $\kappa_o L$ is small. Fig. 3(b) illustrates that this simple model captures the qualitative features of the data. The total time to switch this filter from completely ON to completely OFF is determined by the maximum fluid velocity and the length of the grating. For the device described here, this switching time is 800 ms, which corresponds to a rate of change in the depth of the filter of ∼24 dB/s.

The switching speed increases, of course, as the length of the active area of the fiber decreases and as the speed of the plug increases. Fig. 4, for example, shows the switching of a broad-band (flat wavelength response from 1520 to 1560 nm) attenuator that uses a short (∼5-mm) etched fiber segment (∼13 μm in diameter, formed by etching with hydrofluoric acid). Here, increasing overlap with a high index plug uniformly increases the transmission losses over a relatively wide wavelength range. The data of Fig. 4 show that fluidic tuning results in a filter that has $<\sim$1-dB insertion loss, $>$75-dB dynamic range (instrument limited response), and full switching times of less than ∼30 ms. The response of this system, which uses a machined Teflon spacer, is moderately faster (∼2.5 times) than a comparable device made with molded DER microchannels. We speculate that the slight asymmetry in the ON and OFF switching times observed in Fig. 4 is due to some combination of contact angle hysteresis and flow-induced motion of the fiber.

IV. Conclusion

The tunable microfluidic optical-fiber devices described here may represent an important technology that can complement or even replace certain strain and thermally tuned systems. The electrowetting pumps enable fast low-power ($<$1 mW) tuning that does not require moving parts or mechanical or thermal stresses. The microchannel designs and the single-substrate integration of the electrowetting pump electrodes make this technology easy to integrate with planar waveguides and other micro-optical systems. These and other directions are the subject of current work.

References

[1] P. Mach, C. Kerbage, M. Dolinski, K. W. Baldwin, R. S. Windeler, B. J. Eggleton, and J. A. Rogers, "Tunable microfluidic optical fiber," *Appl. Phys. Lett.*, vol. 80, pp. 4294–4296, June 2002.

[2] P. Mach, T. Krupenkin, S. Yang, and J. A. Rogers, "Dynamic tuning of optical waveguides with electrowetting pumps and recirculating fluid channels," *Appl. Phys. Lett.*, vol. 81, pp. 202–204, July 2002.

[3] C. Kerbage, R. Windeler, B. J. Eggleton, P. Mach, M. Dolinski, and J. A. Rogers, "Tunable devices based on dynamic positioning of micro-fluids in micro-structured optical fiber," *Opt. Commun.*, vol. 204, pp. 179–184, Apr. 2002.

[4] M. W. J. Prins, W. J. J. Welters, and J. W. Weekamp, "Fluid control in multichannel structures by electrocapillary pressure," *Science*, vol. 291, pp. 277–280, Jan. 2001.

[5] A. M. Vengsarkar, P. J. Lemaire, J. B. Judkins, V. Bhatia, T. Erdogan, and J. E. Sipe, "Long period fiber gratings as band-rejection filters," *J. Lightwave Technol.*, vol. 14, pp. 58–65, Jan. 1996.